Lie Group Analysis on Boundary Layer Flow of Nanofluid over a Stretching Sheet with Thermal Radiation

[1]A.K.Pandey, Manoj Kumar, Khilap Singh

[1]*Department of Mathematics, Statistics and Computer Science*
G.B. Pant University of Agriculture and Technology, Pantnagar, India-2263145

Email: alokpandey1@gmail.com, mnj_kumar2004@yahoo.com, singh.khilap8@gmail.com

Abstract: This present paper deals with the study of effect of thermal radiation on steady flow of a nano-fluid past a stretching surface with chemical reaction. The transport equations along with boundary conditions converted into dimensionless form then transformed into a set of coupled ordinary differential equations using similarity transformation generated by Lie group transformations. The physical significance of interesting parameters on the velocity, temperature and concentration profile as well as the local skin friction coefficient, Nusselt number and Sherwood number are thoroughly examined.

Keywords: Chemical reaction, Lie group analysis, Nanofluid, Stretching sheet, Thermal radiation.

2010 Mathematics Subject Classification: 76D; 76D10; 80A20; 82D80

Nomenclature

C_f	skin-friction coefficient
C_w	volume concentration at wall
D_B	Brownian diffusion coefficient
D_T	thermophoretic diffusion coefficient
f	dimensionless velocity of the fluid
g	acceleration due to gravity
h_f	heat transfer coefficient
k_1	rate of chemical reaction
k^*	mean absorption coefficient
k	thermal conductivity of the nanofluid $[Wm^{-1}K^{-1}]$
Le	Lewis number
m	constant
Nr	buoyancy ratio parameter
Nb	Brownian motion parameter
Nt	thermophoresis parameter
Nu	Nusselt number
Pr	Prandtl number
q_r	radiative heat flux [W/m^2]

Ra	Rayleigh number
R	thermal radiation parameter
S	suction/injection parameter
Sh	Sherwood number
T_w	temperature at the wall
T	temperature [K]
u, v	velocities in x; y-directions$[ms^{-1}]$
x, y	axial and perpendicular co-ordinates [m]

Greek Symbols

$\psi(x,y)$	stream function
β	thermal expansion coefficient of the base fluid
ϕ	nanoparticle volume fraction, %
η	similarity variable
γ	chemical reaction parameter
λ	convection parameter
$(C\rho)_f$	heat capacity of the fluid
$(C\rho)_p$	heat capacity of a nanoparticle
ν	kinematic viscosity of the fluid$[m^2s^{-1}]$
κ	thermal conductivity of the fluid $[Wm^{-1}K^{-1}]$
θ	non-dimensional temperature
α	thermal diffusivity
σ^*	Stefan–Boltzmann constant
ρ_f	density of base fluid$[kgm^{-3}]$
ρ_p	density of solid particle $[kgm^{-3}]$

Subscripts

∞	free stream condition
w	condition at the wall
f	base fluid
p	Nanoparticle

Superscript

$'$	derivative with respect to η

1. INTRODUCTION

In the last few decades' nanofluid are widely used in many industrial and technology applications, such as cancer therapy, enery storage, drug delivery, melts of polym ers, paints, asphalts and glues etc. Das [1] studied impact of steady two dimensional MHD boundary layer flow of nanofluid past a convectively heated stretching sheet in the presence of chemical reaction. He found that on increasing the values of chemical reaction parameter the mass transfer rate near the surface rises. Das [2] analyzed the influence of heat

generation/absorption on MHD boundary layer stagnation point flow of nanofluid over a heated stretching sheet with chemical reaction. The effect of MHD boundary layer flow of nanofluid over a stretching surface was made by Ganesh et al. [3]. Hamad and Ferdows [4] investigated the impact of heat generation/absorption on boundary layer stagnation-point flow of nanofluid towards a heated stretching surface in the presence of porous medium and suction/injection. They found that on enhancing the values of Lewis number, the boundary layer thickness reduces for both the cases suction and injection. Haq et al. [5] have discussed the effect of thermal radiation on stagnation point flow of nanofluid over a stretching surface with slip condition and they have seen that heat transfer rate increases with radiation parameter while decreases with increasing values of Lewis number. The effect of solar radiation on unsteady Hiemenz flow of Cu-water nanofluid along a porous wedge surface observed by Kandasamy et al. [6] and they have seen that temperature of the Cu-water nanoparticle reduces with enhancing the values of thermal radiation parameter. Lin et al. [7] investigated the heat transfer flow of nanofluid in the presence of thermal radiation and Marangoni convection flow. Mahmoodi and Kandelousi [8] described the influence of the thermal radiation and Eckert number on two dimensional nanofluid flows through a channel with entropy generation. Pal and Mandal [9] investigated that the impact of thermal radiation on steady two dimensional mixed convection boundary layer stagnation point flow of nanofluid along a stretching/shrinking surface with viscous dissipation and porous medium. Pal et al. [10] analyzed the effect of thermal radiation and heat transfer on two dimensional stagnation point flow of nanofluid over a stretching/shrinking surface in the presence of porous medium. Wubshet et al. [11] examined the MHD nanofluid flow over a stretching sheet in the presence of thermal radiation and slip.
In the present study we analyzed the effects of thermal radiation on steady two dimensional boundary layer flow of nanofluid past a stretching surface. The equations that obtained have been solved in symbolic computation software with the help of Runge-Kutta-Felberg method and shooting technique.The effects of different physical parameters on the velocity,temperature and volume concentration are depicted graphically.

2. MATHEMATICAL FORMULATION

Consider a steady two dimensional natural convection boundary layer flow of a nanofluid along a permeable vertical stretching surface. The direction of flow is the *x*–axis and y-axis is normal to the flow. The surface is contact with a hot fluid at temperature T_w with heat transfer coefficient h_f. The volume fraction C of nanopartical at the surface is C_w and free stream temperature and concentration far from the sheet are T_∞, C_∞ respectively.

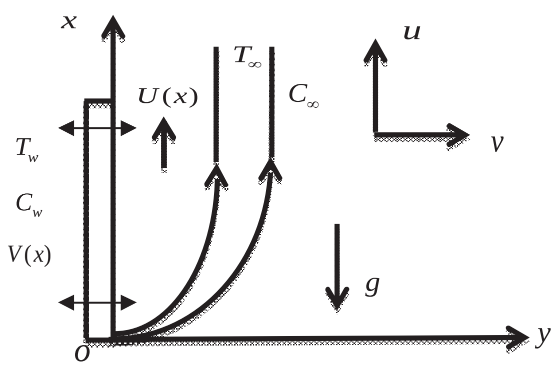

Figure 1 Physical model and coordinate system

Using Oberbeck-Boussinesq approximations, the governing equations for the conservation of the mass, momentum, energy and diffusion can be written in two-dimensional Cartesian coordinate (*x*,*y*) as:

$$u\frac{\partial u}{\partial x}+v\frac{\partial v}{\partial y}=0 \tag{1}$$

$$u\frac{\partial u}{\partial x}+v\frac{\partial v}{\partial y}=\upsilon\left(\frac{\partial^2 u}{\partial y^2}\right)+\left[(1-C_\infty)\rho_{f\infty}\beta g(T-T_\infty)-(\rho_p-\rho_{f\infty})g(C-C_\infty)\right] \tag{2}$$

$$u\frac{\partial T}{\partial x}+v\frac{\partial T}{\partial y}=\alpha\left(\frac{\partial^2 T}{\partial y^2}\right)-\frac{1}{\rho C_p}\frac{\partial q_r}{\partial y}+\tau\left[D_B\frac{\partial C}{\partial y}\frac{\partial T}{\partial y}+\frac{D_T}{T_\infty}\left(\frac{\partial T}{\partial y}\right)^2\right] \tag{3}$$

$$u\frac{\partial C}{\partial x}+v\frac{\partial C}{\partial y}=D_B\left(\frac{\partial^2 C}{\partial y^2}\right)+\frac{D_T}{T_\infty}\left(\frac{\partial^2 T}{\partial y^2}\right)-k_1(C-C_\infty) \tag{4}$$

The related boundary conditions are:

$$u=U(x),\qquad v=V(x),\qquad -k\frac{\partial T}{\partial y}=h_w(T_w-T),\qquad C=C_w,\qquad \text{at } y=0$$

$$u\to 0,\qquad T\to T_\infty,\qquad C\to C_\infty.\quad \text{as } y\to\infty \tag{5}$$

Where u and v are the velocity components along *x* and *y*-axis respectively, Further, ν is the kinematic viscosity of base fluid, ρ is the density of fluid, D_T is the thermophoretic diffusion coefficient, τ is the ratio of the effective heat capacity of the nanoparticle material to the base fluid, α is the thermal diffusivity, D_B is the Brownian diffusion coefficient, k_1 is the rate of chemical reaction, k is the effective thermal conductivity, h_w is the heat transfer coefficient and q_r is the radiative heat flux. The suffixes w and ∞ indicate surface and ambient conditions, x and y represent coordinate axes.

The stream wise velocity and suction/blowing velocity are taking as [1].

$$U(x)=ax^m,\ V(x)=V_0x^{(m-1)/2}$$

Here a is constant and for steady case take as unit value, m is the power-law exponent (constant), V_0 is the velocity of suction if $V_0<0$ and injection if $V_0>0$. With the help of Rosseland approximation, the radiative heat flux is

$$q_r=-\frac{4\sigma^*}{3k^*}\frac{\partial T^4}{\partial y} \tag{6}$$

Here σ^* is the Stefan-Boltzman constant and k^* is the mean absorption coefficient, and T^4 is the linear sum of temperature and it can be expanding with help of Taylor series about T_∞.

$$T^4=T_\infty^4+4T_\infty^3(T-T_\infty)+6T_\infty^2(T-T_\infty)^2+\dots \tag{7}$$

Ignoring higher order terms of $(T-T_\infty)$ onwards of equation (7) we get:

$$T^4\cong 4T_\infty^3T-3T_\infty^4 \tag{8}$$

Solving equations (6) and (8) we get:

$$q_r=-\frac{16T_\infty^3\sigma^*}{3k^*}\frac{\partial T}{\partial y} \tag{9}$$

In usual way a stream function $\psi(x,y)$ and non-dimensional similarity variables are defined as

$$u=\frac{\partial\psi}{\partial y},\ v=-\frac{\partial\psi}{\partial x} \tag{10}$$

$$\theta(\eta)=\frac{T-T_\infty}{T_w-T_\infty},\ \phi(\eta)=\frac{C-C_\infty}{C_w-C_\infty} \tag{11}$$

Using the equations (9) - (11), then the system of Equations (1) - (5) becomes:

$$\frac{\partial\psi}{\partial y}\frac{\partial^2\psi}{\partial x\partial y}-\frac{\partial\psi}{\partial x}\frac{\partial^2\psi}{\partial y^2}-\nu\left(\frac{\partial^3\psi}{\partial y^3}\right)=\left(1-\phi_\infty\right)\rho_{f\infty}\beta g\theta\Delta\theta-\left(\rho_p-\rho_{f\infty}\right)g\phi\Delta\phi \tag{12}$$

$$\frac{\partial\psi}{\partial y}\frac{\partial\theta}{\partial x}-\frac{\partial\psi}{\partial x}\frac{\partial\theta}{\partial y}=\alpha\frac{\partial^2\theta}{\partial y^2}+\frac{16T_\infty^3\sigma^*}{(\rho C)_f 3\kappa^*}\frac{\partial^2\theta}{\partial y^2}+\tau\left[D_B\Delta\phi\frac{\partial\phi}{\partial y}\frac{\partial\theta}{\partial y}+\frac{D_T}{T_\infty}\Delta\theta\left(\frac{\partial\theta}{\partial y}\right)^2\right] \tag{13}$$

$$\frac{\partial\psi}{\partial y}\frac{\partial\phi}{\partial x}-\frac{\partial\psi}{\partial x}\frac{\partial\phi}{\partial y}=D_B\frac{\partial^2\phi}{\partial y^2}+\frac{D_T\Delta\theta}{T_\infty\Delta\phi}\frac{\partial^2\theta}{\partial y^2}-k_1\phi \tag{14}$$

Associated boundary conditions are:

$$\frac{\partial\psi}{\partial y}=x^m,\quad \frac{\partial\psi}{\partial x}=-V_0x^{\frac{(m-1)}{2}},\quad -k\frac{\partial\theta}{\partial y}=h_w\left(1-\theta\right),\quad \phi=1,\quad \text{at y=0,}$$

$$\frac{\partial\psi}{\partial y}\to 0,\quad \theta\to 0,\quad \phi\to 0,\quad \text{as } y\to\infty. \tag{15}$$

here $\Delta\theta=T_w-T_\infty$ and $\Delta\phi=C_w-C_\infty$.

2.1. Lie group transformation and similarity solutions

$$\Gamma: x^*=xe^{\varepsilon\alpha_1}, y^*=ye^{\varepsilon\alpha_2}, \psi^*=\psi e^{\varepsilon\alpha_3}, u^*=ue^{\varepsilon\alpha_4}, v^*=ve^{\varepsilon\alpha_5}, \theta^*=\theta e^{\varepsilon\alpha_6}, \phi^*=\phi e^{\varepsilon\alpha_7}\ \}. \tag{16}$$

$$e^{\varepsilon(\alpha+2\alpha_2-2\alpha_3)}\left(\frac{\partial\psi^*}{\partial y^*}\frac{\partial^2\psi^*}{\partial x^*\partial y^*}-\frac{\partial\psi^*}{\partial x^*}\frac{\partial^2\psi^*}{\partial y^{*2}}\right)=ve^{\varepsilon(3\alpha_2-\alpha_3)}\frac{\partial^3\psi^*}{\partial y^{*3}}+e^{-\varepsilon\alpha_6}\left(1-\phi_\infty\right)\rho_{f\infty}\beta g\Delta\theta$$
$$-e^{\varepsilon\alpha_7}\left(\rho_p-\rho_{f\infty}\right)g\phi\Delta\phi. \tag{17}$$

$$e^{\varepsilon(\alpha_1+\alpha_2-\alpha_3-\alpha_6)}\left(\frac{\partial\psi^*}{\partial y^*}\frac{\partial\theta^*}{\partial x^*}-\frac{\partial\psi^*}{\partial x^*}\frac{\partial\theta^*}{\partial y^*}\right)=\left(\alpha+R\right)e^{\varepsilon(2\alpha_2-\alpha_6)}\frac{\partial^2\psi^*}{\partial y^{*2}}+$$
$$\tau\begin{bmatrix}D_B\Delta\phi e^{\varepsilon(2\alpha_2-\alpha_6-\alpha_7)}\frac{\partial\phi^*}{\partial y^*}\frac{\partial\theta^*}{\partial y^*}\\ +e^{\varepsilon(2\alpha_2-\alpha_6)}\frac{D_T}{T_\infty}\Delta\theta\left(\frac{\partial\theta}{\partial y}\right)^2\end{bmatrix} \tag{18}$$

$$e^{\varepsilon(\alpha_1+\alpha_2-\alpha_3-\alpha_7)}\left(\frac{\partial\psi^*}{\partial y^*}\frac{\partial\phi^*}{\partial x^*}-\frac{\partial\psi^*}{\partial x^*}\frac{\partial\phi^*}{\partial y^*}\right)=D_Be^{\varepsilon(2\alpha_2-\alpha_7)}\frac{\partial^2\phi}{\partial y^{*2}}+\frac{D_T\Delta\theta}{T_\infty\Delta\phi}e^{\varepsilon(2\alpha_2-\alpha_6)}\frac{\partial^2\theta^*}{\partial y^{*2}}-k_1e^{-\varepsilon\alpha_7}\phi \tag{19}$$

The system of equation (17) - (19) always invariant under the Lie group transformations (16) The following expressions obtained between the parameters:

$$7\alpha_1+2\alpha_2-2\alpha_3=3\alpha_2-\alpha_3=\alpha_2-\alpha_3=-\alpha_6=-\alpha_7;$$
$$\alpha_1+\alpha_2-\alpha_3-\alpha_6=2\alpha_2-\alpha_6=2\alpha_2-\alpha_6-\alpha_7=2\alpha_2-2\alpha_6;$$
$$\alpha_1+\alpha_2-\alpha_3-\alpha_7=2\alpha_2-\alpha_7=2\alpha_2-\alpha_6=-\alpha_7; \tag{20}$$

From this relation, we finally obtained $\alpha_2=\frac{1}{4}\alpha_1=\frac{1}{3}\alpha_3,\ \alpha_6=\alpha_7=0$. Hence the boundary conditions are $\alpha_4=m\alpha_1=\frac{1}{2}\alpha_1,\ \alpha_5=\frac{m-1}{2}\alpha_1=-\frac{1}{4}\alpha_1,$ as $m=\frac{1}{2}$ is taken.

With the help of these, boundary condition becomes:

$$\frac{\partial\psi^*}{\partial y^*}=x^{*^{1/2}},\quad \frac{\partial\psi^*}{\partial x^*}=-V_0x^{*^{-1/4}},\quad -k\frac{\partial\theta^*}{\partial y^*}=h_w\left(1-\theta^*\right),\quad \phi^*=1,\quad \text{at } y^*=0,$$

$$\frac{\partial \psi^*}{\partial y^*} \to 0, \qquad \theta^* \to 0, \quad \phi^* \to 0, \qquad \text{as } y^* = \infty \tag{21}$$

Thus the group of transformations (16) converted into

$$\Gamma : x^* = xe^{\varepsilon\alpha_1},\ y^* = ye^{\varepsilon\alpha_1/4},\ \psi^* = \psi e^{3\varepsilon\alpha_1/4},\ u^* = ue^{\varepsilon\alpha_1/2},\ v^* = ve^{-\varepsilon\alpha_1/4}, \theta^* = \theta,\ \phi^* = \phi. \tag{22}$$

Using Taylor's series, we are getting the following relations:

$$x^* - x = x\varepsilon\alpha_1,\ y^* - y = y\varepsilon\,\alpha_1/4,\ \psi^* - \psi = 3y\varepsilon\,\alpha_1/4,\ u^* - u = u\varepsilon\,\alpha_1/2,\ v^* - v = -v\varepsilon\,\alpha_1/4,$$

$$\theta^* = \theta,\ \phi^* = \phi. \tag{23}$$

The auxiliary equations for finding the similarity variable are

$$\frac{dx}{x\alpha_1} = \frac{dy}{y\,\alpha_1/4} = \frac{d\psi}{3\psi\,\alpha_1/4} = \frac{du}{u\,\alpha_1/2} = \frac{dv}{-v\,\alpha_1/4} = \frac{d\theta}{0} = \frac{d\phi}{0}. \tag{24}$$

Now solving above equations, we obtained:

$$y^* x^{*^{-1/4}} = \eta, \qquad \psi^* = x^{*^{3/4}} f(\eta), \qquad \theta^* = \theta(\eta), \qquad \phi^* = \phi(\eta). \tag{25}$$

Using similarity transformation (25), the governing Equations (17)-(19) are converted into a set of non-linearly ordinary differential equations defined as follows:

$$f''' + \frac{1}{\Pr}(0.75 ff'' - 0.5 f'^2) + Ra(\theta - Nr\phi) = 0, \tag{26}$$

$$(1+R)\theta'' + 0.75 \Pr f\theta' + \Pr Nb\theta'\phi' + \Pr Nt\theta'^2 = 0, \tag{27}$$

$$\phi'' + 0.75 Lef\phi' + \frac{Nt}{Nb}\theta'' - \gamma\phi = 0 \tag{28}$$

and boundary conditions are

$$f = S, \qquad f' = 1, \qquad \theta' = -\lambda(1-\theta), \qquad \phi = 1, \quad \text{at } \eta = 0,$$

$$f' = 0, \quad \theta = 0, \quad \phi = 0, \quad \text{as } \eta = \infty \tag{29}$$

here f, θ and ϕ are the non-dimensional velocity, temperature and volume concentration of nanoparticle respectively. The prime denotes differentiation with respect to η and the dimensionless parameters, Prandtl number $(\Pr)$, local Rayleigh number (Ra), Lewis number (Le), Buoyancy ratio parameter (Nr), Brownian motion parameter (Nb), thermophoresis parameter (Nt), thermal radiation parameter (R), chemical reaction parameter (γ), the suction/injection parameter (S), the surface convection parameter (λ), heat transfer coefficient (h_w) are defined as follows:

$$\Pr = \frac{\nu}{\alpha}, \quad Ra = \frac{(1-\phi_\infty)\beta g\Delta\theta}{\nu\alpha}, \quad Le = \frac{\nu}{D_B}, \quad Nr = \frac{(\rho_p - \rho_{f\infty})\Delta\phi}{(\rho_{f\infty}\beta\Delta\theta(1-\phi_\infty))}, \quad Nb = \tau D_B \Delta\phi,$$

$$Nt = \tau D_T \frac{\Delta\theta}{T_\infty}, \quad R = \frac{16\sigma * T_\infty^3}{3k^* k}, \quad \gamma = k_1\frac{U}{\nu},, \quad S = -\frac{4V_0}{3}, \quad \lambda = \frac{h_w}{k}x^{1/2}, \quad h_w = cx^{-1/4}.$$

The parameters of physical interest are the skin friction coefficient (rate of shear stress), Nusselt number (rate of heat transfer) Nu and Sherwood number (rate of mass transfer) Sh are defined as

$$C_f = \frac{\mu}{\rho_f U}\left(\frac{\partial u}{\partial y}\right)_{y=0} = -\mathrm{Re}_x^{-1/2} f'', \qquad Nu = -\frac{x}{T_w - T_\infty}\left(\frac{\partial T}{\partial y}\right)_{y=0} = -\mathrm{Re}_x^{1/2}(1+R)\theta'(0),$$

$$Sh = -\frac{x}{C_w - C_\infty}\left(\frac{\partial C}{\partial y}\right)_{y=0} = -\mathrm{Re}_x^{1/2}\phi'(0).$$

here $Re_x = \dfrac{xU}{\nu_f}$ is the local Reynolds number.

The reduced Nusselt number and the reduced Sherwood number are defined as follows:

$$Nur = Re_x^{-1/2}\, Nu = -\left(1+R\right)\theta'\left(0\right), \quad Shr = Re_x^{-1/2}\, Sh = -\phi'\left(0\right). \tag{30}$$

3. RESULTS AND DISCUSSION

The transformed equations 26-29 subject to boundary conditions (29) were integrated numerically using the Runge-Kutta-Fehlberg method with shooting technique to obtain the missing values of $f''\left(0\right), \theta'\left(0\right)$ and $\phi'\left(0\right)$, for some values of the governing parameters. In order to study the effects of the radiation parameter, buoyancy parameter and Prandtl number on the velocity, temperature and concentration profiles. The other values of the other parameters are fixed as $Ra = 1,\ Nb = Nt = 1.0,\ Le = 3.0,\ S = 0.8,\ \lambda = 1,\ \gamma = 0.5.$ Then the non-dimensional velocity, temperature and concentration profiles are illustrated in Figures 2-10. Figure 2 depicts that the effect of thermal radiation parameter R on fluid velocity for $Nr = 0.5,\ Nt = 1,\ \lambda = 1,\ \gamma = 0.5,\ Le = 3,\ S = 0.8,\ Pr = 1$. This Figure show that on increasing the values of R the velocity of nanoparticle regularly increases then the boundary layer thickness of velocity rises. Figure 3 reveals that on increasing the values of thermal radiation parameter R, temperature of the nanoparticle increases. Due to this reason thermal boundary layer thickness increases and surface temperature also growing. Figure 4 demonstrates the impact of thermal radiation parameter R on nanoparticle volume concentration ϕ. It is observed from graph that on enhancing the values of thermal radiation parameter R, the concentration of nanoparticle slowly decreases. Due to this reason concentration boundary layer thickness thin.

The influence of buoyancy parameter on fluid velocity, temperature and concentration for $R = 1, Nt = 1, \lambda = 1, \gamma = 0.5, Le = 3, S = 0.8, Pr = 1$ are shown in Figures 5-7. Figure 5 illustrates that on increasing the values of Nr velocity of nano-particle continuously reduces. From figugure 6 it is clear that on enhancing the values of buoyancy ratio parameter temperature of nanoparticle regularly growing.Fig.7 reveals that on enhancing the values of buoyancy parameter Nr volume concentration of nanoparticle continously increases due to this reason boundary layer thickness of the nanoparticle rises.

Figures 8-10 display the influence of Prandtl number on velocity, temperature and volume concentration of nano-particle for $R = 1,\ Nt = 1,\ \lambda = 1,\ \gamma = 0.5,\ Le = 3,\ S = 0.8,\ Nr = 1$. On growing Prandtl number, velocity of the nanoparticle significantly increases as shown in Figure 8. It is observed from Figure 9 that temperature of the nanoparticle regularly reduces on increasing the values of Pr. Due to this reason boundary layer thickness reduces. Figure 10 illustrates that concentration of nanoparticle decreases with increasing the values of Prandtl number. This is due to the fact that nanoparticle concentration boundary layer becomes thin.

Table 1 Variation of reduced skin friction coefficient, reduced Nusselt number and reduced Sherwood number in the case of $R = 1,\ Nt = 1,\ \lambda = 1,\ \gamma = 0.5,\ Le = 3,\ S = 0.8,\ Pr = 1.$

Nr	$-f''(0)$	$-\theta'(0)$	$-\phi'(0)$
0.5	0.7438902	0.2663170	2.5406919
2	1.1980099	0.2620970	2.5144419
4	1.8374499	0.2556500	2.4744919
6	2.53149	0.24776	2.426549

It is clear from Table3 that the values of reduced Nusselt number $\mathrm{Re}_x^{-1/2} Nu$, skin friction coefficient $\mathrm{Re}_x^{1/2} C_f$ decreases and reduced Sherwood number $\mathrm{Re}_x^{-1/2} Sh$ rises on enhancing the values of thermal radiation parameter R. The impact of buoyancy ratio parameter Nr and Prandtl number $\Pr$ on the of reduced Nusselt number $\mathrm{Re}_x^{-1/2} Nu$, skin friction coefficient $\mathrm{Re}_x^{1/2} C_f$ and reduced Sherwood number $\mathrm{Re}_x^{-1/2} Sh$ when the stretching surface is heated convectively are shown in Table1, 2. It is noticed from the table heat transfer rate regularly reduces with increasing the values Nr and increases with increasing in the Prandtl number. While mass transfer rate decreases when buoyancy ratio parameter Nr increases and increases on growing the values of Prandtl number $\Pr$. The value of reduced skin friction coefficient $\mathrm{Re}_x^{1/2} C_f$ rises with increasing the values of Nr and decreases with increasing $\Pr$.

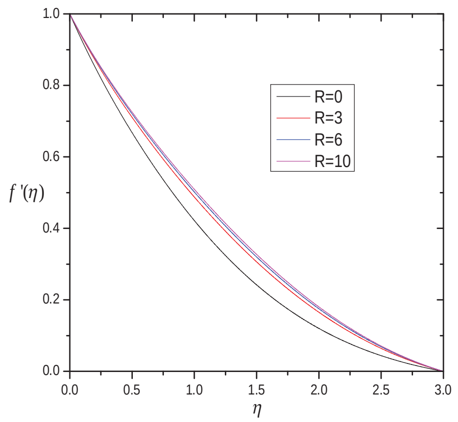

Fig.2 Velocity profiles of different values of R.

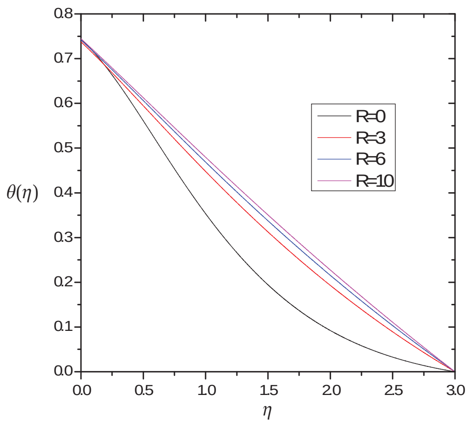

Fig.3 Temperature profiles of different values of R.

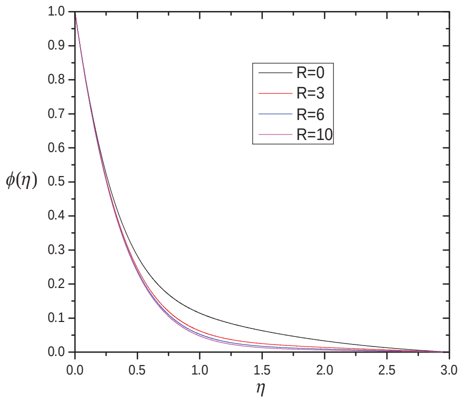

Fig.4 Concentration profiles of different values of R.

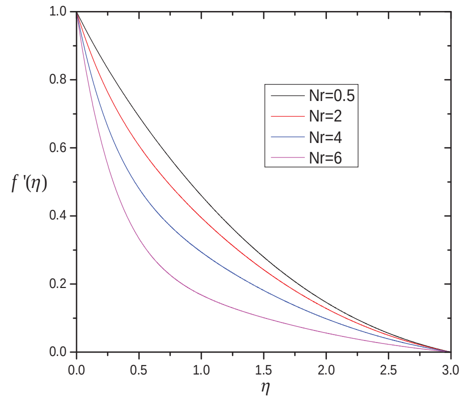

Fig. 5 Velocity profiles of different values of Nr.

Table 2 Variation of the reduced skin friction coefficient reduced Nusselt number and reduced Sherwood number in the case of $R=1,\ Nt=1,\ \lambda=1,\ \gamma=0.5,\ Le=3,\ S=0.8,\ Nr=1.$

Pr	$-f''(0)$	$-\theta'(0)$	$-\phi'(0)$
0.05	12.4206393	0.2490148	2.2063531
0.07	8.9927985	0.2488478	2.2493839
0.2	3.3976048	0.2495378	2.4003340
0.4	1.8511293	0.2533515	2.4798931
0.6	1.3208501	0.2579015	2.5096931

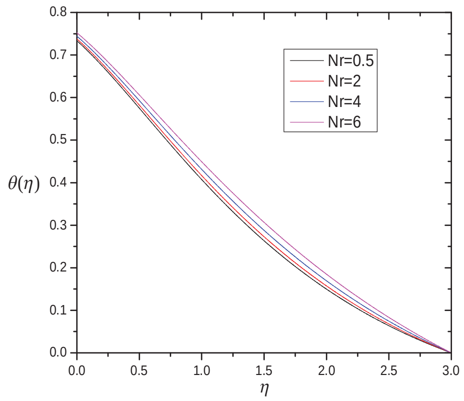

Fig. 6 Temperature profiles of different values of Nr.

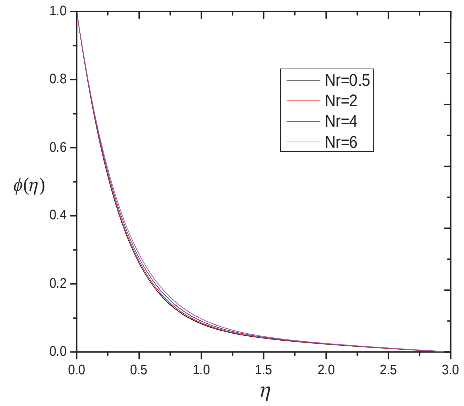

Fig.7 Concentration profiles of different values of Nr.

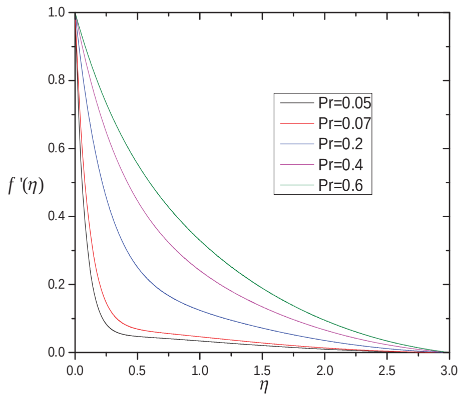

Fig.8 Velocity profiles of different values of *Pr*.

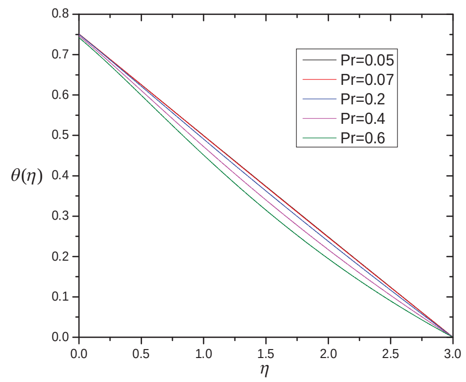

Fig.9 Temperature profiles of different values of *Pr*.

Table 3 Variation of the reduced skin friction coefficient reduced Nusselt number and reduced Sherwood number in the case of $\Pr=1,\ Nt=1,\ \lambda=1,\ \gamma=0.5,\ Le=3,\ S=0.8,\ Nr=1.$

R	$-f''(0)$	$-\theta'(0)$	$-\phi'(0)$
0	0.7985519	0.2564204	2.5364116
3	0.6988152	0.2623204	2.5594116
6	0.6749015	0.2581703	2.5719189
10	0.6621915	0.2555704	2.5792892

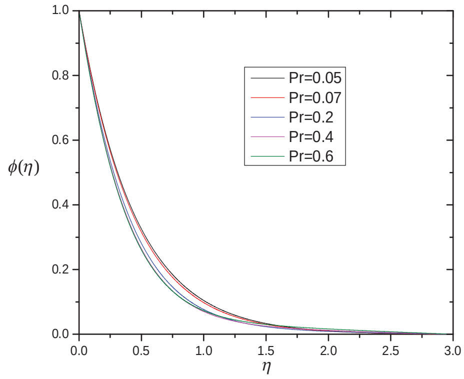

Fig.10. Concentration profiles of different values of Pr.

4. CONCLUSIONS

The influence of thermal radiation on two-dimensional steady boundary layer flow of nanofluid along a heated permeable stretching surface is investigated by the use of lie group transformations to change the boundary layer equations into non-linear ordinary partial differential equations. The impact of various physical parameters like thermal radiation parameter R, buoyancy ratio parameter Nr and Prandtl number $\Pr$ on reduced skin friction coefficient $\mathrm{Re}_x^{1/2} C_f$, Nusselt number $\mathrm{Re}_x^{-1/2} Nu$ and reduced Sherwood number $\mathrm{Re}_x^{-1/2} Sh$ are studied and presented its tabuleted values. Thus, the following conclusion was obtained:

- Velocity, temperature profile of the nanoparticle increases with increasing in the thermal radiation parameter and concentration profile of nanoparticle reduces.
- Temperature and concentration profile of nanoparticle rises with raising the values of buoyancy ratio parameter and reduces with increasing the values of Prandtl number.
- The reduced skin friction coefficient $\mathrm{Re}_x^{1/2} C_f$ decreases with increasing in the thermal radiation parameter and Prandtl number and it increases with increase of the buoyancy ratio parameter Nr.
- The reduced Nusselt number $\mathrm{Re}_x^{-1/2} Nu$ decreases with growing in the buoyancy ratio parameter Nr.
- The reduced Sherwood number $\mathrm{Re}_x^{-1/2} Sh$ enhance with growing thermal radiation parameter R and Prandtl number $\Pr$ whereas it reduces with increase of the buoyancy ratio parameter Nr.

References:

[1] Das K., Lie group analysis for nanofluid flow past a convectively heated stretching surface, Applied Mathematics and Computation 221: 547–557, 2013.

[2] Das K., Lie group analysis of stagnation-point flow of a nanofluid, Microfluid Nanofluid 15: 267–274, 2013.

[3] Ganesh N.V., Ganga B., Hakeem A. K. A., Lie symmetry group analysis of magnetic field effects on free convective flow of a nanofluid over a semi-infinite stretching sheet, Journal of the Egyptian Mathematical Society 22: 304–310, 2014.
[4] Hamad M. A. A., Ferdows M., Similarity solution of boundary layer stagnation-point flow towards a heated porous stretching sheet saturated with a nanofluid with heat absorption/generation and suction/blowing: A lie group analysis, Commun Nonlinear Sci Numer Simulat 17: 132–140, 2012.
[5] Haq R. U., Nadeem S., Khan Z. H., Akbar N. S., Thermal radiation and slip effects on MHD stagnation point flow of nanofluid over a stretching sheet, Physica E 65: 17–23, 2015.
[6] Kandasamy R., Muhaimin I., Khamis A. B., Roslan R. B., Unsteady Hiemenz flow of Cu-nanofluid over a porous wedge in the presence of thermal stratification due to solar energy radiation: Lie group transformation, International Journal of Thermal Sciences 65: 196-205, 2013.
[7] Lin, Y., Zheng, L., Zhang, X., Radiation effects on Marangoni convection flow and heat transfer in pseudo-plastic non-Newtonian nanofluids with variable thermal conductivity, International Journal of Heat and Mass Transfer 77: 708–716, 2014.
[8] Mahmoodi M., Kandelousi Sh., Effects of thermophoresis and Brownian motion on nanofluid heat transfer and entropy generation, Journal of Molecular Liquids 211: 15–24, 2015.
[9] Pal D., Mandal G., Mixed convection-radiation on stagnation point flow of nanofluid over a stretching/shrinking sheet in a porous medium with heat generation and viscous dissipation, Journal of Petroleum Science and Engineering 126:16-25, 2015.
[10] Pal D., Mandal G., Vajravelu K., Flow and heat transfer of nanofluids at a stagnation point flow over a stretching/shrinking surface in a porous medium with thermal Radiation, Applied Mathematics and Computation 238: 208–224, 2014.
[11] Wubshet, I., Bandari, S., MHD boundary layer flow and heat transfer of a nanofluid over a stretching permeable stretching sheet with velocity, thermal and solutal slip boundary conditions, Computers & Fluids. 75: 1–10, 2013.